Wettability of Hydrogenated Tetrahedral Amorphous Carbon

F. Piazza[1*], G. Morell[2,3]

[1] Pontificia Universidad Católica Madre y Maestra, Santo Domingo, P.O. Box 2748, Dominican Republic

[2] Department of Physics, University of Puerto Rico, San Juan, P.O. Box 23343, PR 00931, USA

[3] Institute for Functional Nanomaterials, University of Puerto Rico, San Juan, P.O. Box 23343, PR 00931, USA

The wettability and surface energy of hydrogenated amorphous carbon films (a-C:H) elaborated by distributed electron cyclotron resonance plasma were studied by contact angle measurements in relation to composition, structure and topography. Tetrahedral a-C:H (ta-C:H) showed relatively high water contact angle (CA) up to 82.3°, and low surface energy (E_s), down to 25.3 mJ/m^2. Hydrophobicity was found to increase with the intensity of the ion bombardment and with the tetrahedral character. A decrease of the dispersive component is responsible of the decrease of surface energy with substrate bias. Low mass-density polymer-like a-C:H (PLC) present also a relatively high hydrophobicity with high water CA, up to 76.7°, and low surface energy values, down to 32.1 mJ/m^2. Hydrophobicity is interpreted as resulting from a surface layer rich in sp^2-carbon for ta-C:H and rich in C-H bonds for PLC.

* Corresponding author. *E-mail address:* fabricepiazza@pucmm.edu.do (F. Piazza)

1. Introduction

Hydrogenated amorphous carbon films (a-C:H) containing a high fraction of sp^3-bonds between carbon have received extensive interest [1]. Such films are called hydrogenated tetrahedral amorphous carbon films (ta-C:H). This is due to a combination of superlative diamond-like properties, that are promoted by sp^3-bonding between carbon. These properties include high hardness and large Young modulus, low coefficient of friction, high wear and corrosive resistance, atomic smoothness, infrared-transparency, high refractive index, chemical inertness, biocompatibilty, low electron affinity, high electrical resistivity, and lack of magnetic response [1]. In addition, the films can be grown at near room temperature with reasonable growth rate (typically 50 nm/min) and are much cheaper to produce than rougher nanocrystalline diamond that typically requires substrate temperatures above 400°C [2,3]. Recently the growth of diamond nanocrystals on polymer at lower temperature, down to 250°C, was achieved, but growth rate is presently too low for practical applications [4,5]. Therefore ta-C:H is a competitive and cost-effective engineering material with widespread potential applications, mainly as protective, antiwear and anti-corrosion hard-coating in areas such as magnetic [1,6,7,8,9,10,11] and optical storage devices [12,13,14], optical windows [1], medical implants and tools [15], and more recently, as anti-wear and anti-stick templates for nanoimprint lithography (NIL) [16]. It is also a potential candidate to be used as alternative material to silicon in micro-electromechanical devices (MEMS) [11,17,18,19,20,21].

Ta-C:H has been elaborated by high electron density plasma enhanced chemical vapor deposition (PECVD) techniques from a hydrocarbon precursor, such as plasma beam source (PBS) [22], electron cyclotron wave resonance source (ECWR) [23,24] and distributed electron cyclotron resonance (DECR) plasma [25,26]. The sp^3-content, mass-density, Young's modulus, and hardness, are typically of ~75%, 2.4 g/cm^3, 300 GPa, and 45 GPa,

respectively. Hydrogen content varies between 20 and 30 at. %. Carbon-carbon sp^3-bonding is promoted by the deposition from a source of medium-energy ions. Typically the energy per carbon atom carried by an impinging hydrocarbon ion is ~150 eV [1,27]. Also carbon-carbon sp^3-bonding increases with the ion flux for a constant ion energy [25].

Surface energy and wettability are among the key ta-C:H properties for the above-mentioned applications. Surface energy affects surface properties and interfacial interactions such as adsorption, wetting, adhesion, and friction [28,29]. Low surface energy is necessary for applications where friction needs to be minimized [30,31]. In biocompatible coating applications, the surface properties and controllable hydrophobicity is of great importance in controlling cell attachment [15]. In data storage technologies, these properties, that determine the interfacial interactions between carbon and lubricant film, must be carefully controlled to minimize lubricant loss from the disk surface and simultaneously ensure adequate lubricant mobility during operation [32]. In nanoimprint lithography (NIL), ta-C:H is considered as a promising anti-stick protective hard coating to increase lifetime of expensive nanostructured templates that suffer from serious damage after a number of imprint cycles, especially in case of hot-embossing technique [16]. Here, low surface energy is very important to prevent the adhesion of the viscous polymer or liquid resin [16,33]. In MEMS devices, hydrophobic ta-C:H with low surface energy may be one of the best candidates for the application of stiction-reducing coating [11,17,18,19,20,21].

Typically, a surface is considered hydrophobic if its contact angle with water is above 70°, and hydrophilic if it is below 70° [34]. Small E_s gives large CA value. Contact angle data for extensively-characterized ta-C:H are scarce. Relatively high water CA values in the range 70-80º were reported for ta-C:H elaborated from ion beam source [35]. Typically, for a-C:H, $40 \leq E_s \leq 44$ mJ/m^2 and $55 \leq CA \leq 70^o$ [32,36,37,38,39,40]. The surface energy of a-C:H can be modified by incorporating other elements in the amorphous carbon matrix that also modify

structure and stress. The surface energy of a-C:H was found to increase from 41 mJ/m^2 for pure a-C:H to 52 mJ/m^2 upon oxygen addition [38], and to decrease to extremely low values, between 19 and 24 mJ/m^2, upon Si, F or Fe addition [32,38,38,41,42]. However, achieving very low surface energy in this way often results in the lost of diamond-like character [37]. Recently, a-C:H films prepared by heat-treatment of polymer have been shown to have relatively high water CA values, between 88 and 92°, and very low surface energy, down to 25 mJ/m^2 [29], which is similar to films containing iron [42]. It was found that roughness has no effect on contact angle and that the decrease in surface energy was related to an increase in sp^2-carbon content [29].

Despite of its great importance in various applications, wettability and surface energy have not been extensively investigated in relation to film composition, structure, and topography. Variation in contact angle measurements conditions, surface energy calculation, and material structure make comparison between studies unreliable. Details on the origin of wettability properties of carbon materials remain unclear.

This paper reports on the surface energy properties from contact angle measurements of a-C:H and ta-C:H films deposited by DECR plasma from C_2H_2 at various substrate bias and pressure. The relations between contact angle, surface energy, composition, structure, and topography are discussed.

2. Experimental details

The synthesis experimental details were previously published [25,26]. Briefly, the films were grown on Si <100> and polycarbonate substrates using a DECR plasma reactor described in Ref. [43]. The samples were placed 27 cm away from the bottom of the magnetic racetracks. A microwave power P_{MW} of 800 W at a frequency of 2.45 GHz was applied to the C_2H_2 gas used as precursor. The plasma pressure (pressure during plasma operation), P, was

varied from 0.1 to 1.1 mTorr (from 13.3 to 146.6 mPa). The negative bias, V_0, applied to the 300 mm diameter substrate holder was varied within the range 25-600 V using a power supply operating at 13.56 MHz. The bias was kept constant during deposition by an automatic modulation of the RF power. Near room temperature deposition was attained by employing water-cooled substrate holder. For the experimental conditions employed, the temperature at the surface of the substrate holder during deposition remained below 140°C, the glass temperature of polycarbonate (PC). No damage of the PC substrates was observed after deposition. PC was only used here to test the temperature during deposition. For film characterization, films were deposited on Si substrates. Prior to deposition, the Si substrates were exposed to Ar plasma cleaning for 5 min (P_{MW} = 800 W, P = 0.5 mTorr, V_0 = –50 V).

The films were previously characterized by a wide range of complementary techniques including multiple-wavelength Raman spectroscopy (MWRS), laser induced surface acoustic waves (LISAW), electron energy loss spectroscopy (EELS), electron diffraction (ED), and Fourier transform infrared spectroscopy (FTIR) [25,26,43,44,45,46]. The hydrogen content was determined from nuclear reaction analysis (NRA) using the resonance at 6.385 MeV of the reaction: $^{15}N + {}^{1}H \rightarrow {}^{12}C + {}^{4}He + \gamma$ [25,44]. The thickness was determined from spectroscopic ellipsometry (SE) [25,44,43]. It is between 70 and 190 nm for the films analysed. The mass-density was deduced from the SE and NRA data [25,44,43].

The surface topography was investigated using a Nanoscope III Atomic Force microscope (Digital Instruments) in air operating in tapping mode [26]. Before the measurements, the samples were stored in high vacuum. Etched silicon cantilevers and tips were used (TESP series probes from Veeco). The oscillation frequency of the cantilever was typically around 375 kHz. The tip had a radius of curvature below 10 nm. The cantilever was routinely replaced to avoid imaging artifacts due to tip aging. The root mean square (rms)

roughness R_q, was calculated from scans performed on a 500×500 nm^2 area with 512 lines of resolution.

Contact angle was measured by the sessile-drop method at 20°C under atmospheric conditions using a contact angle goniometer (Model 120 from Ramé-hart Instrument). Beside de-ionized water, a second liquid, 99.8 % anhydrous ethylene glycol (from Aldrich), was employed to calculate the polar and dispersion components of surface energy from Owen and Wendt equation [47]. All measurements were conducted on aged samples following extended storage period under ambient conditions since it is known that surface wettability of fresh a-C:H evolved with time [32]. Prior to measurement, the samples were cleaned by acetone in an ultrasonic bath and then dried by nitrogen gas. A droplet with a volume of 2 μl was released onto the surface of the sample from a syringe needle. Photographs of the drops were taken by a charge coupled device (CCD) camera after a waiting period of 3 to 8 s. Contact angle was measured at least three times (at different locations). Reproducibility is typically below ±1.5°.

3. Results

3.1. Composition and structure

It is possible to tune the composition and structure of carbon films by varying the ion flux and energy. A detailed study was previously reported [25]. The main results obtained are summarized below.

The diamond–like character is tuned by changing the ion flux (i.e. the pressure) for constant ion energy (i.e. substrate bias). When the ion flux is increased above 2×10^{15} ions cm^{-2} s^{-1} the sp^3-fraction (C-C bonds), the cross-linking between carbon atoms and the diamond-like character increase due to ion energy loss and transfer process [25,26]. For a constant substrate bias V_0 of −150 V, the mass-density, Young's modulus, and hardness reach a maximum value of ~2.5 g/cm^3, ~280 GPa, and 45 ~GPa, respectively, and the hydrogen content reaches a minimum of 26 at. % for the maximum ion flux ϕ_+ of ~6.3×10^{15} ions cm^{-2} s^{-1} [25]. This is characteristic of ta-C:H. When the ion flux is decreased below 2×10^{15} ions cm^{-2} s^{-1}, a-C:H and polymer-like carbon (PLC) are elaborated. The carbon incorporation decreases and there is an increase in hydrogen incorporation which is enhanced at low pressure (0.1 mTorr), by a high production of hydrogen radicals in the plasma. The mass–density decreases below 1.6 g/cm^3. There is an increase in the C–H sp^3-fraction rather than C–C sp^3 fraction. The cross-linking between carbon is low and the films become more polymer-like. Films with mass-density as low as 1.2 g/cm^3 can be synthesized at low pressure (0.1 mTorr) [25]. The mass-density of a-C:H and PLC is typically in the range of 1.5 to 1.8 g/cm^3 and $\leq$1.5 g/cm^3, respectively.

In addition, for a constant ion flux and pressure, the mass-density and Young's modulus reach a maximum at a substrate bias of –300 V, and the hydrogen content is minimized (Fig. 1). For taC:H deposited at 0.5 mTorr (which corresponds to ϕ_+~5.2×10^{15} ions cm^{-2} s^{-1}, value close to the maximum ion flux attainable in the present experimental conditions), the mass-

density first increases with $|V_0|$, reach a maximum when $|V_0|$ ~300 V and then slightly decreases with a further increase of the bias to $|V_0|$ =600 V (Fig. 1c). The maximum mass-density is reached when the carbon atoms carried by $C_2H_x^+$ ions, which are the predominant impinging ions, undergo a subplantation process with ~150 eV energy. This is in good agreement with previous experimental results and their interpretation by the subplantation model [1,27]. For 0.5 mTorr the maximum of mass-density and Young's modulus are of 2.3 g cm^{-3} and 250 GPa, respectively.

MWRS showed that the films grown at the maximum or near maximum ion flux and at negative substrate bias ranging between 150 and 500 V are ta-C:H [25]. Their spectra are characteristic of ta-C:H [48,49]. There is no clear dip at ~1500 cm^{-1} between the D and G band, and a weak T band can be observed. In addition the UV G band position is higher than 1600 cm^{-1} while at the same time its width and dispersion are relatively large. The G band frequency, full width at half maximum (FWHM) and dispersion vary from ~1617 to 1600 cm^{-1}, 180 to 156 cm^{-1}, and 0.29 to 0.20 cm^{-1}/nm, respectively, within the bias range considered [25]. These features distinguish ta-C:H from other forms of a-C:H. Their tetrahedral character was confirmed by the mean bond length and mean bond angle values obtained from ED [25]. On the other hand, MWRS showed that the low mass-density films grown with ion flux below ~2×10^{15} ions cm^{-2} s^{-1} and negative substrate bias below 150 V are polymer-like films (PLC) [25]. In their UV Raman spectra there is a clear dip at ~1500 cm^{-1} between the D and G band. The T band is very weak. The UV G band position is still higher than 1600 cm^{-1} as for ta-C:H but at the same time its width (typically ~91 cm^{-1}) and dispersion are low (typically ~0.1 cm^{-1} /nm) [25].

In this paper, we will focus on three series of characteristic carbon films deposited using various substrate bias: ta-C:H and a-C:H deposited at 0.5 mTorr (with ϕ_+~ 5.2×10^{15} ions cm^{-2} s^{-1}), ta-C:H and a-C:H deposited at 0.9 mTorr (with ϕ_+~2×10^{15} ions cm^{-2} s^{-1}) and very low

mass-density (1.2 g/cm^3) PLC deposited at 0.1 mTorr (with ϕ_+~2×10^{15} ions cm^{-2} s^{-1}). Further details about the arrangement of sp^2-carbon atoms were obtained by MWRS. The following conclusions were drawn [25] about the films hereby studied:

1. The films contain sp^2-clusters and chains.

2. The increase of the ion flux induces a decrease in clustering and increase in tetrahedral character.

3. The increase of the negative substrate bias induces an increase in clustering.

4. An increase in the hydrogen incorporation reduces clustering.

5. Ta-C:H and a-C:H deposited at 0.5 mTorr and 0.9 mTorr contain more disorder than low-density (1.2 g/cm^3) PLC deposited at 0.1 mTorr.

6. The disorder decreases with the increase of the negative substrate bias.

In conclusion, ion flux and energy, and plasma pressure have a strong influence on film composition and structure.

3.2. Surface topography

A detailed surface topography study was previously reported [26]. Fig. 1(a) shows the rms roughness R_q as a function of negative substrate bias for a-C:H and ta-C:H deposited at 0.5 mTorr. Thickness is of 150 nm. Fig. 2 shows typical 3D AFM surface images of characteristic films, labeled S1, S2, S3, S4. S1 and S2 correspond to 1.7 g/cm^3 dense a-C:H (Fig. 2(a)) and 2.3 g/cm^3 dense ta-C:H deposited at 0.5 mTorr (Fig. 2(b)). S3 corresponds to 2.2 g/cm^3 dense ta-C:H deposited at 0.9 mTorr (Fig. 2(c)). Finally, S4 corresponds to 1.2 g/cm^3 dense PLC deposited at 0.1 mTorr (Fig. 2(d)). Table 1 summarizes corresponding films properties in relation with process parameters. We consider that thickness values are within the range where roughness is thickness-independent according to ref. 50.

Fig. 2(b) and 1(a) show that ta-C:H grown at 0.5 mTorr using a negative bias within the range 150-500 V, are atomically smooth. R_q varies from 0.16 to 0.08 nm. These values are comparable to results for ECWR ta-C:H films [50].

As it can be seen on Fig. 2(a) and 1(a), the roughness of lower mass-density (1.7 g/cm^3) a-C:H films grown at 0.5 mTorr and at -25 V bias is significantly higher. It is of 0.25 nm (sample S1). In the case of PLC films of very low mass-density (1.2 g/cm^3), elaborated at low pressure (0.1 mTorr) and ion flux (φ_+~2×10^{15} ions cm^{-2}s^{-1}), such as S4, which have been shown to contain transpolyacetylene (TPA) chains [45,46], the roughness value are even higher, within the range 0.29-0.44 nm. For instance Rms roughness of S4 is of 0.329 nm (Fig. 2(d)). These last two results are in good agreement with data reported for a-C:H films deposited at low power by conventional RF-PECVD and ECR-RF techniques [51].

The surface topography of 2.2 g/cm^3 dense ta-C:H deposited at 0.9 mTorr (φ_+~1.9×10^{15} ions cm^{-2} s^{-1}), that is to say at higher pressure, and under -300 V substrate bias, such as S3 (Fig. 2c), is different from that of ta-C:H deposited at 0.5 mTorr (φ_+~5.2×10^{15} ions cm^{-2} s^{-1}) using a negative bias within the range 150-500 V (Fig. 2b). Randomly distributed hillocks are visible on a very smooth surface, similar to the surface characteristic of ta-C:H deposited at 0.5 mTorr. The hillocks are typically 1 to 2 nm high and 40 to 100 nm wide. Their surface density is relatively low, of the order of 6.4×10^9 cm^{-2}, when compared to the ion dose (1.9×10^{15} ions cm^{-2} s^{-1}). The hillocks increase the overall rms roughness of the film (R_q=0.20 nm). Their origin was discussed elsewhere [26]. They were interpreted as resulting from the interference that takes place between high energy shock waves that are triggered by the overlap of collision cascades produced by $C_4H_x^+$ ions inducing non linear effects at high pressure [26].

In conclusion, ion flux and energy, and plasma pressure have a strong influence on surface topography.

3.3. Contact angle and surface energy

Fig. 3A shows contact angle, CA, as a function of negative substrate bias for water (squares) and for ethylene glycol (triangles) for film deposited at 0.5 mTorr. Fig. 1d shows the corresponding evolution of surface energy. Fig. 3B details the corresponding evolution of surface energy polar and dispersion components. Fig. 4A to 4D show the typical optical micrographs of a de-ionized water drop on the surface of sample S1, S2, S3, and S4, respectively (Table 1). Although films of different structure are involved, it is interesting to compare our data with previous studies on characteristic carbon materials. Table 2 provides such comparison.

Fig. 3A and Fig. 4B show that the surface of ta-C:H prepared at 0.5 mTorr with a negative bias within the range 150-500 V have a hydrophobic nature with water CA in the range of 77.5 to 82.3°. This is significantly higher than data typically reported for a-C:H [32,38,37,38,39,40,52,53] (section 1) but it is in the same range as for ta-C:H elaborated from ion beam source (section 1) [35] and for ta-C elaborated by filtered cathodic vacuum arc (FCVA) technique [42,54,55,56] (Table 2). Our data are significantly lower than values reported in Ref. [29] for a-C:H prepared by heat-treatment of polymer precursor within the range 88.1 to 91.7°. Interestingly, our results are higher than the CA value of 73±3° reported for nanocrystalline diamond, NCD [57], which coincides with that of a polished (110) plane of single-crystal diamond after ultrasonic cleaning and heating up to 150 °C [58].

Water CA first significantly increases with $|V_0|$, from ~71.3 to 82.3° between 25 and 200 V, and then slightly decreases to 77.5° with a further increase of the bias to $|V_0|$ =600 V (Fig. 3A). Ethylene glycol CA follows the same trends (Fig. 3A).

Water CA for 2.1 to 2.2 g/cm^3 mass-density ta-C:H deposited at 0.9 mTorr with negative substrate bias ranging from 250 to 500 V is slightly but systematically lower than ta-C:H deposited at 0.5 mTorr, 75.8 ≤CA≤ 77.8° (Fig. 4C).

Water CA for lower mass-density a-C:H films, typically 1.7 to 1.8 g/cm^3, is significantly lower than for ta-C:H. Typically, 71.3 ≤CA≤ 74.4° (Fig. 4A). Interestingly, in the case of polymeric films of very low mass-density (1.2 g/cm^3), containing TPA chains [45,46], water CA value is higher and closer within the range reported for ta-C:H deposited at 0.9 mTorr. Typically, 75.8 ≤CA≤ 76.7° (Fig. 4D).

The trends observed and described above for water are reproduced for ethylene glycol, but with lower CA values. Also, they are logically closely related to the surface energy data.

The surface energy of ta-C:H prepared at 0.5 mTorr is relatively low: 25.3≤E_s≤ 30.6 mJ/m^2 (Fig. 1d and Table 2). Interestingly, the data range is similar to results reported in Ref. [29] for a-C:H prepared by heat treatment of polymer. The surface energy of ta-C:H films prepared at –200 V is as low as 25.3 mJ/m^2, which is the value reported for a-C:H prepared at 900°C in Ref. [29] and for amorphous carbon containing Fe or Al, a-C:Fe and a-C:Al, respectively [16,24] (Table 2). A significantly higher surface energy of 41.5 mJ/m^2 was reported for ta-C:H elaborated from ion beam source [35].

ta-C:H films with 2.1 to 2.2 g/cm^3 mass-density deposited at 0.9 mTorr with negative substrate bias ranging from 250 to 500 V do not attain such low surface energy value although the data are in the same range as that of ta-C:H deposited at 0.5 mTorr, 29.2 ≤E_s≤ 31.7 mJ/m^2.

For a-C:H and ta-C:H deposited at 0.5 mTorr, the surface energy first significantly decreases with $|V_0|$, from ~33.9 to 25.3 mJ/m^2 between 25 and 200 V, and then slightly increases to 30.3 mJ/m^2 with a further increase of the bias to $|V_0|$ =600 V (Fig. 1d).

The surface energy for 1.7 to 1.8 g/cm^3 mass-density a-C:H films, is slightly higher than for ta-C:H. Typically, 32 ≤E_s≤ 34 mJ/m^2 (Fig. 1). This is lower than the values typically reported for a-C:H, between 40 and 44 mJ/m^2 (section 1). Interestingly, in the case of polymeric films of very low mass-density (1.2 g/cm^3), containing TPA chains, the surface

energy values are lower and similar to those of ta-C:H deposited at 0.9 mTorr (typically, 31 $\leq E_s \leq$ 32.1 mJ/m^2).

The surface energy is considered to be composed by two contributions: a high dispersion component, E_δ, and a lower polar component, E_p. In the case of ta-C:H deposited at 0.5 mTorr, typically, 8.6 $\leq E_p \leq$ 14.2 mJ/m^2 while 13.9 $\leq E_\delta \leq$ 22 mJ/m^2 (Fig. 3B). The corresponding data for ta-C:H deposited at 0.9 mTorr, are similar, typically, 11.1 $\leq E_p \leq$ 12.7 mJ/m^2 and 16.4 $\leq E_\delta \leq$ 20.4 mJ/m^2.

In the case of 1.7 to 1.8 g/cm^3 mass-density a-C:H films, both components tend to be slightly higher than for ta-C:H, typically, 12.7 $\leq E_p \leq$ 15.2 mJ/m^2 and 18.7 $\leq E_\delta \leq$ 19.5 mJ/m^2 (Fig. 3B). In the case of polymeric films of very low mass-density (1.2 g/cm^3), containing TPA chains, E_δ and E_p values are lower and similar to those of ta-C:H deposited at 0.9 mTorr (typically, E_p~11.2-11.5 mJ/m^2 and 19.5 $\leq E_\delta \leq$ 20.9 mJ/m^2).

Both surface energy components evolve with substrate bias (Fig. 3B). For a-C:H and ta-C:H deposited at 0.5 mTorr, E_p first significantly decreases with $|V_0|$, from 15.2 to 8.6 mJ/m^2 between 25 and 300 V, and then slightly increases to 11.0 mJ/m^2 with a further increase of the bias to $|V_0|$ =600 V. E_δ first decreases from ~18.7 to 13.8 mJ/m^2 between 25 and 150 V, slightly increases to 15.4 mJ/m^2 for $|V_0|$ =250 V, then increases significantly to 22 mJ/m^2 with a further increase of the bias to $|V_0|$ =300 V, and finally slightly decreases to 19.3 mJ/m^2 with a further increase of the bias to $|V_0|$=600 V (Fig. 3B). Fig. 3B shows that the reduction in dispersion component is responsible for the reduction in total surface energy with the substrate bias. Interestingly, an analogous trend was observed as a function of synthesis temperature for a-C:H prepared from polymers [29].

Our dispersive and polar components data for ta-C:H are relatively low and high, respectively, as compared to corresponding data for a–C:H prepared by heat-treatment of polymer precursor [29] (Table 2). In that case, 1.7 $\leq E_p \leq$ 3.8 mJ/m^2 and 21.1 $\leq E_\delta \leq$ 37.3, as

compared to our data, $8.6 \leq E_p \leq 14.2$ mJ/m^2 and $14 \leq E_\delta \leq 22$ mJ/m^2. Our polar component is in the same range as that reported for FCVA ta-C, $9 \leq E_p \leq 13$ mJ/m^2, although in those cases E_δ is significantly higher, $31 \leq E_\delta \leq 31.7$ mJ/m^2 [42,55]. In comparison to our data, ta-C:H from Ref. [35] also present similar polar component, of 10.5 mJ/m^2, but significantly higher dispersive components, of 31 mJ/m^2. Lower polar component, of 4.4 mJ/m^2 and higher dispersive component, of 45.6 mJ/m^2, were reported for NCD [57].

4. Discussion

Various factors may have impact on the surface energy and wettability: surface chemical bonds, structure, surface topography, and adsorbates. The overall wettability is determined by the interplay of these factors, some of them promoting hydrophobicity whereas others, enhancing hydrophilicity. Variation in contact angle measurements conditions, surface energy calculation, material structure, and lack of structure information makes comparison between studies unreliable. The details of the origin of wettability properties of carbon materials remain unclear. However the effects of some factors are known.

Surface hydrogenation of microcrystalline diamond [59], and nanocrystalline diamond [57] enhances the hydrophobic character. This is associated with the saturation of dangling bonds by hydrogen forming strong C-H bonds and leading to a weaker interaction between film and water [59]. A reconstruction of the surface to form sp^3-hybridized state of carbon induced by the adsorption of hydrogen is also thought to contribute to a decrease in the dipole moment of the surface and the enhancement of hydrophobicity [59,60,61,62,63,64]. This is supported by the decrease of the polar component with hydrogenation [65].

On the other hand, surface oxygenation of microcrystalline diamond [59], nanocrystalline diamond [57], and ta-C [56], makes the surface more reactive due to the formation of oxygen-containing functional groups serving as active centers of water wetting. The polar

component of surface energy, which is responsible for donor–acceptor interactions at the solid–liquid interface, increases with oxygenation [65]. Furthermore, for ta-C, it was shown, that higher oxygen adsorption is enabled with sp^3-surface carbon whereas lower oxygen coverage is compatible with sp^2-surface carbon [56]. Again, the adsorption of oxygen induces an increase in polar surface energy component [56,66].

Also, it is known that, as a result of the deposition mechanism, the surface atoms of ta-C and ta-C:H have dangling bonds [1]. It was shown that their surface reconstructs to remove some of these dangling bonds for surface energy minimization reason. This is usually done by the formation of sp^2 sites. This was confirmed by theoretical works [67,68,69,70,71,72] and experimental results [1,73,74,75,76,43]. This reconstruction operates as well in NCD which present sp^2-rich surface [77].

Finally, sp^2-rich surfaces present higher contact angle than sp^3-rich surfaces [78,79]. Water CA for natural diamond single crystals (111) and graphite (0001) of 35º and 78º, respectively, were reported [80].

These findings together with the analysis of composition, structure (section 3.1) and surface topography (section 3.2) are employed to understand our results on wettability (section 3.3).

We start with the analysis of the potential relationship between surface roughness, hydrogen content, mass-density, and wettability. ta-C:H films prepared at 0.5 mTorr using a negative bias within the range 150-500 V have a constant hydrogen content of 22.5 at.% and are all atomically smooth. A typical 3D AFM image of ta-C:H film prepared at –200 V is shown in Fig. 2B. R_q varies from 0.16 to 0.08 nm within the range considered, but there is no obvious trend. On the contrary, there are some continuous variations in wettability and surface energy as described above (Fig. 3 and section 3.3). Films deposited at 200 and 300 V present the same roughness, of 0.08 nm, but a significant variation in surface energy, of 5.2

mJ m^{-2}. Also, it is possible to obtain a similar surface energy for films with different surface topography and roughness, and hydrogen content. For instance, the roughness and hydrogen content of films deposited at 0.1 mTorr and –400 V are relatively high, of 0.33 nm and 32 at. %, respectively, while the roughness and hydrogen content of films deposited at 0.5 mTorr and –300 V are relatively low, of 0.08 nm and 22.4 at. %, respectively (Fig. 2D and Fig. 2B). However, both types of films present surface energy values very close, of 31.1 and 30.6 mJ m^{-2}, respectively. Although the surface roughness may have an impact on contact angle and surface energy, our results show that there is no direct relationship between roughness and surface energy. They also show that there is no direct relationship between hydrogen content and surface energy.

Fig. 1 shows that surface energy significantly decreases when the negative substrate bias is increased from 25 to 200 V while hydrogen content and roughness decrease, and mass-density increases. This corresponds to a structure change from polymer-like type film to diamond-like type (see section 3.1). Fig. 5 shows the relation between water contact angle and mass-density. It shows that apart from 1.2 g/cm^3 mass-density films containing TPA chains, the contact angle tends to increase with mass-density although there is no direct relationship between them.

We tentatively interpret the hydrophobicity of ta-C:H elaborated at 0.5 mTorr as resulting from the reconstruction of the surface by forming sp^2-sites to minimize energy following Ref. [1, 43,67,68,69,70,71,72,73,74,75,76]. Various elements support this interpretation:

1. The formation of ta-C:H films at 0.5 mTorr is characterized by an intense ion bombardment that promotes the formation of dangling bonds (section 3.1) [25,26]. This is supported by the evolution of disorder analyzed by MWRS (section 3.1). Since polar component is relatively low, we consider that absorption of oxygen at the surface from

dangling bonds is low. Therefore dangling bonds must have rearranged to lower surface energy.

2. Similar contact angle data and polar component values were reported for FCVA ta-C and ta-C:H obtained from ion beam (section 3.3). In these two cases, film formation is also characterized by an intense ion bombardment [35,42,54,55,56]. The polar component was related to sp^2-bonds, which are more polar than C-H bonds.
3. ta-C:H elaborated at 0.9 mTorr present smaller contact angle and higher surface energy values as compared to ta-C:H obtained at 0.5 mTorr (section 3.3). The ion flux is significantly lower at 0.9 mTorr than at 0.5 mTorr: $\sim 2\times10^{15}$ ions cm^{-2} s^{-1} as compared to $\sim 5.2\times10^{15}$ ions cm^{-2} s^{-1} (section 3.1) [25,26]. Less dangling bonds are formed at 0.9 mTorr than at 0.5 mTorr.
4. The increase of contact angle and decrease in surface energy when the negative substrate bias is increased from 25 to 200 V, and when mass-density is increased from 1.7 to 2.3 g/cm^3 (section 3.3), correspond to an increase in the tetrahedral character of the films (section 3.1 and 3.2). We assume that, when the tetrahedral increases, the reorganization of the surface into sp^2-rich layer is enhanced. This results in a decrease in the surface mass-density, although bulk-mass density increases, and decrease in the dispersive component (Figure 3). It was proposed that the reduction in the mass-density of the surface results in a drop in lattice energy and in the dispersive component of the surface energy [66,38,81,82,56,32]. In the case of a-C:H containing Si, a higher surface energy dispersive component was associated to a higher cross-linking in the network structure [83]. This is also consistent with the observation a significant decrease in dispersive component of a-C:H film after annealing, which was related to the formation of nanocrystalline graphite during annealing [84]. Note that the other possible scenario would be to have a surface

layer rich in sp^3-carbon. This would promote adsorption of oxygen and would induce an increase of polar component. This is not the case so this hypothesis is ruled out.

5. The surface energy of ta-C:H elaborated at 0.5 mTorr and prepared at –200 V is as low as 25.3 mJ/m^2, which is the value reported for a-C:Fe and a-C:Al (section 3.3) [16,24]. In this case, it was shown that the incorporation of metal elements induces an increase in sp^2-content (section 1). We may expect in this case the presence of sp^2-rich surface layer.

The origin of the hydrophobicity of lower mass-density (~1.2 g/cm^3) PLC is different. As compared to ta-C:H, these films are characterized by higher hydrogen content, and lower cross-linking between carbon (section 3.1 and section 3.2). The hydrophobic character is interpreted as resulting from a surface layer rich in C-H bonds as in the case of microcrystalline diamond and NCD for which the surface was exposed to hydrogenation treatment [59,57]. Various elements support this interpretation:

1. PLC films are elaborated at low plasma pressure, 0.1 mTorr where the ion flux is lower (see section 3.1) and where there is a high production of H radicals [44]. There is a higher incorporation of hydrogen. Dangling bonds are mainly passivated by hydrogen [44]. We propose that this passivation prevents in part the formation of a sp^2-rich surface layer.
2. High CA and low surface energy values were reported for a-C:H prepared by heat-treatment of polymer precursor. These a-C:H films are polymer-like as clearly indicated by the C-H stretching band in FTIR spectra, which present well-defined vibration components, as our PLC elaborated at 0.1 mTorr.

Our data on polar and dispersive components further support our interpretation of the results. Considering that sp^2-bonds are more polar than C-H bonds, the higher polar component and lower dispersive component for ta-C:H elaborated at 0.5 mTorr as compared to corresponding data for a–C:H prepared by heat-treatment of polymer precursor (see section 3.3) support the hypothesis of the presence of a surface layer richer in sp^2-carbon in the case

of ta-C:H than for a–C:H prepared by heat-treatment of polymer precursor. In the case of low mass-density PLC, the presence of TPA chains may explain the relatively high polar component, so that hydrogenated sp^2-carbon may be responsible for the hydrophobic properties of the films. In contact with oxygen, polar functional groups like –OH or – COOH may be formatted at the surface and improve the interaction and wettability by polar liquids. This may explain the difference in wettability between ta-C:H and PLC.

Finally, higher dispersive component as compared to our ta-C:H, for FCVA ta-C, ta-C:H from Ref. [35] is interpreted as resulting from differences in cross-linking between carbon atoms in the first case, and also between carbon and hydrogen in the second case. Further study is necessary to characterize the bonding at the surface layer.

4. Conclusion

In summary, wettability and surface energy of a-C:H and ta-C:H films elaborated by DECR plasma from C_2H_2 precursor were studied by contact angle measurements in relation to composition, structure and topography. ta-C:H films have relatively high water contact angle, $77.5 \leq CA \leq 82.3°$, and low surface energy, $30.6 \leq E_s \leq 25.3$ mJ/m^2. Hydrophobicity increases with the intensity of the ion bombardment, and with tetrahedral character. A decrease of the dispersive component is responsible of the decrease of surface energy with bias. Low mass-density polymer-like a-C:H (PLC) present also a high hydrophobicity with $75.8 \leq CA \leq 76.7°$ and $31 \leq E_s \leq 32.1$ mJ/m^2. Hydrophobicity is interpreted as resulting from a surface layer rich in sp^2-carbon for ta-C:H and rich in C-H bonds for PLC. No direct relationship was found between wettability, surface roughness, hydrogen content, or mass-density. The hydrophobic properties of ta-C:H elaborated in this work and its tunability may be of great interest for various applications such as MEMS, magnetic and optical storage

technology, medical implants and tools, and nanoimprint lithography. Relatively high hydrophobicity can be obtained without incorporation of foreign elements.

Acknowledgements

The authors would like to thank, from the University of Puerto Rico, Puerto Rico: L. Fonseca for access to an atomic force microscope, and A. González-Berríos for helpful discussions. This work was supported in part by the European Community (DIAMCO Brite-EuRam Contract N° BRPR-CT98-0749), by the NSF (award EPS-0223152), by NASA (Grant N° NCC3-1034), by the University *Pontificia Universidad Católica Madre y Maestra*, Dominican Republic (2007-2008 Grants for Research "*Fondos Concursables 2007-2008*") and the State Secretary of Higher Education, Science and Technology (SEESCYT) of the Dominican Republic (2007 FONDOCYT program).

Table Captions

1. Mass-density, Hydrogen content, RMS roughness (R_q), water contact angle, ethylene glycol contact angle, total surface free energy (E_S), surface energy polar component (E_p), and surface energy dispersion component (E_δ) for different type of films elaborated at different negative substrate bias and plasma pressure.

2. Comparison of water contact angle, surface energy (E_s), and polar (E_δ) and dispersive (E_d) surface energy components for characteristic carbon thin films.

Figure Captions

1. AFM RMS roughness, R_q, (a), hydrogen content (b), mass-density (c), and surface energy (d), as a function of negative substrate bias (plasma pressure of 0.5 mTorr). Thickness is within the 140-190 nm range.

2. Typical 3D AFM images of S1, S2, S3, S4 (see table 1). RMS roughness, R_q, is indicated.

3. Contact angle for water (circles) and for ethylene glycol (squares) (A), total surface energy (triangles), polar component (circles), and dispersion component (squares) (B), as a function of negative substrate bias (plasma pressure of 0.5 mTorr).

4. Typical optical micrograph of a dionized water drop on the surface of S1, S2, S3, S4 (see table 1). Contact angles are indicated.

5. Water contact angle as a function of mass-density.

FIG. 1. F. PIAZZA et al.

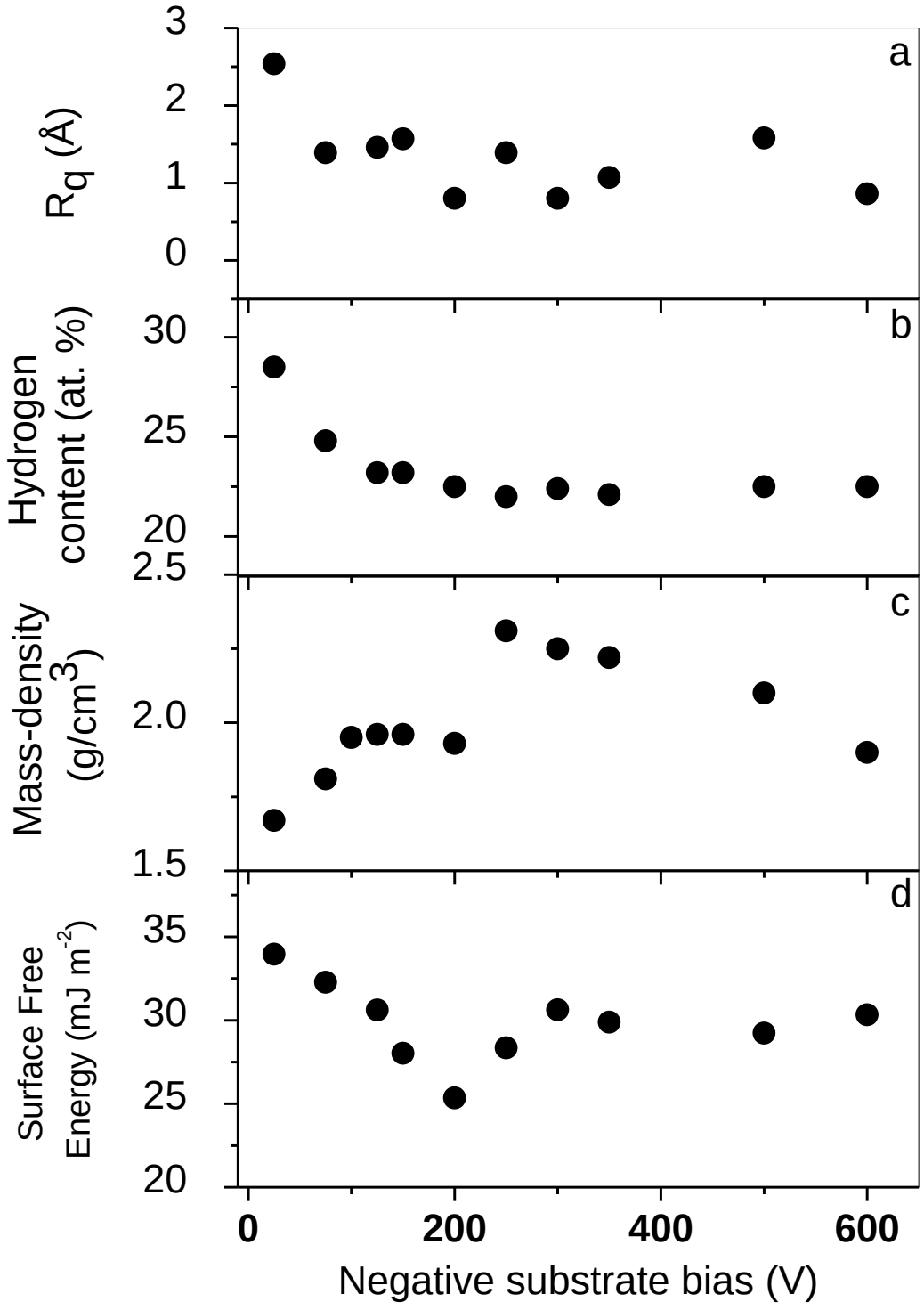

FIG. 2. F. PIAZZA et al.

A) S1; R_q = 2.5 Å

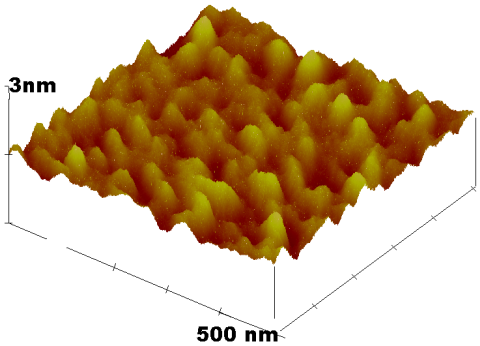

B) S2; R_q = 0.8 Å

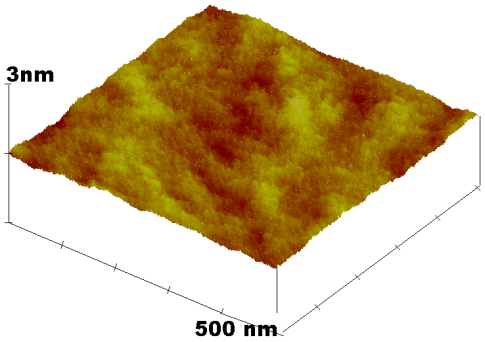

C) S3; R_q = 2.0 Å

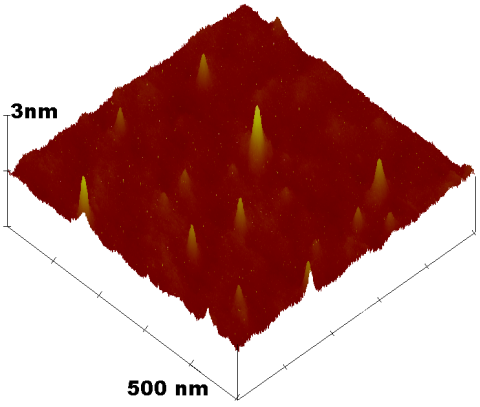

D) S4; R_q = 3.3 Å

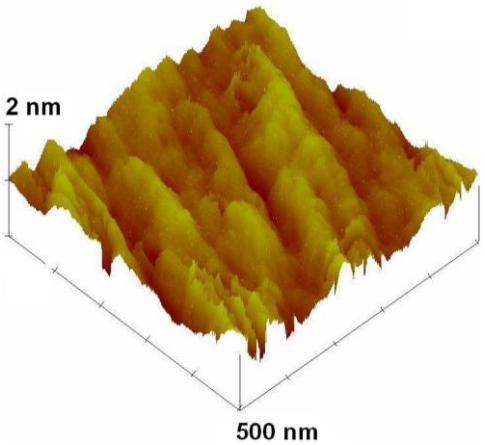

FIG. 3. F. PIAZZA et al.

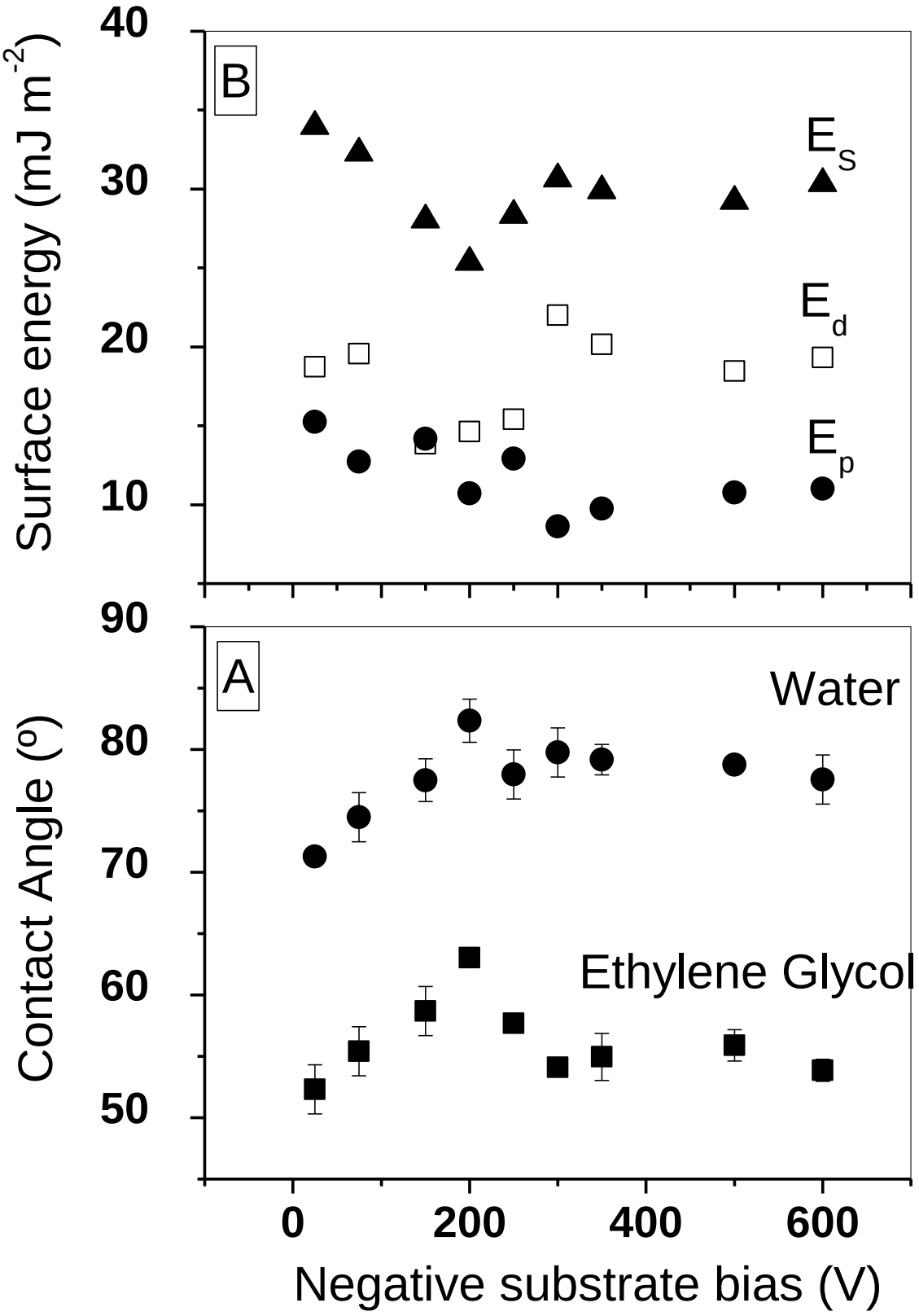

FIG. 4. F. PIAZZA et al.

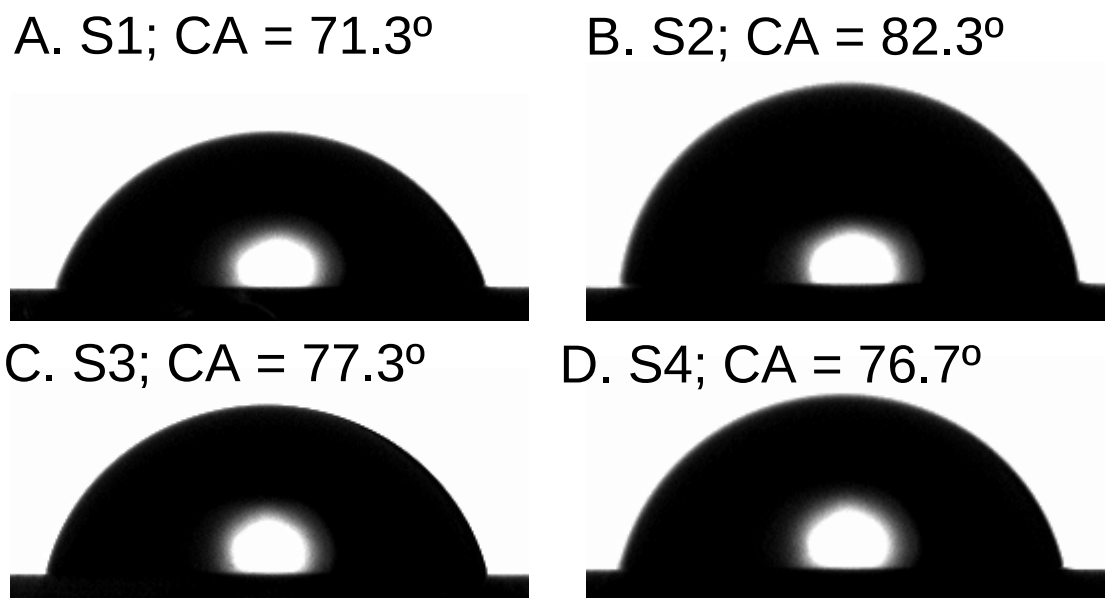

FIG. 5. F. PIAZZA et al.

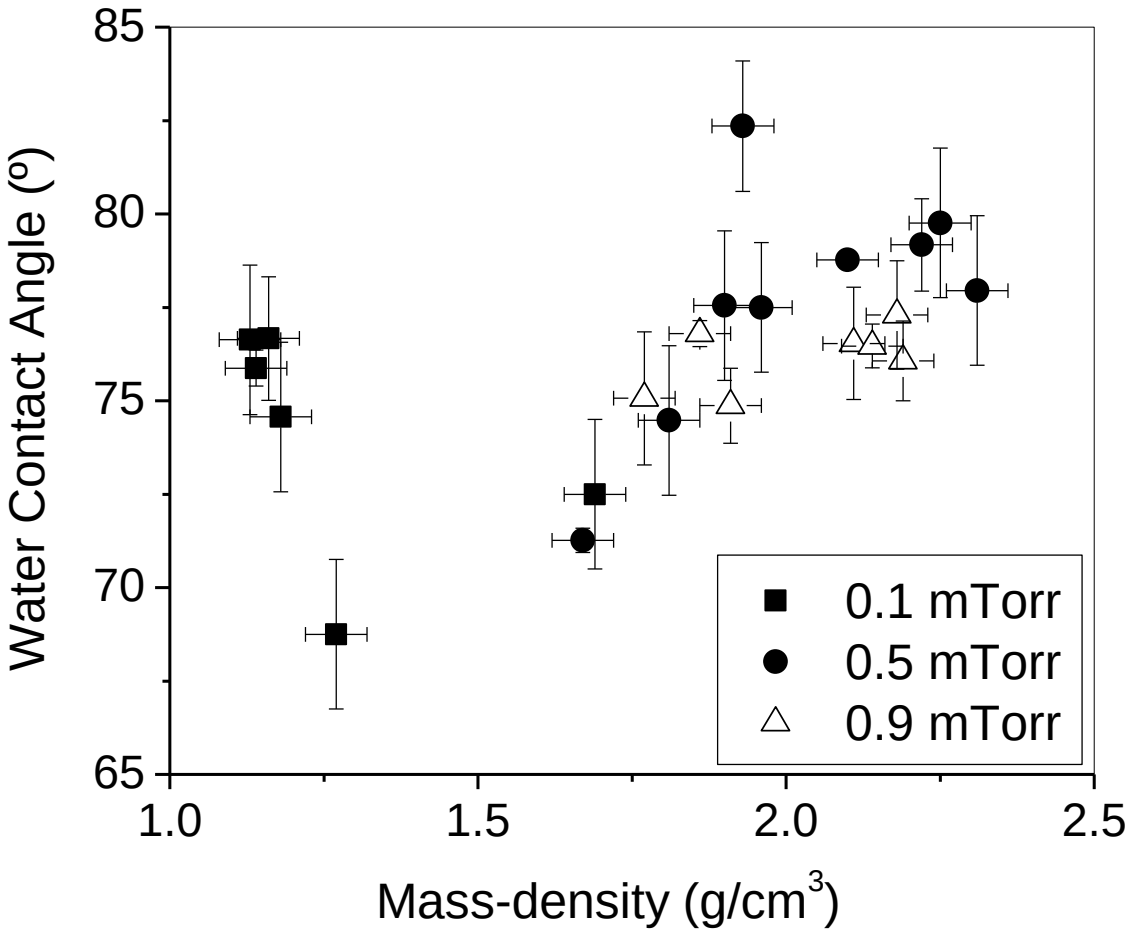

TABLE 1. F. PIAZZA et al.

Number	type	Pressure (mTorr)	Bias (V)	Thickness (nm)	Mass-density (g/cm^3)	H content (at. %)	R_q (Å)	Water CA (º)	$C_2H_4(OH)_2$ CA (º)	E_S (mJ m^{-2})	E_p (mJ m^{-2})	E_δ (mJ m^{-2})
S1	a-C:H	0.5	- 25	150	1.7	28	2.5	71.3	52.3	33.9	15.2	18.7
S2	Ta-C:H	0.5	- 200	150	2.3	22	0.8	82.3	63.0	25.3	10.7	14.6
S3	Ta-C:H	0.9	- 300	120	2.2	23	2.0	77.3	56.1	29.2	12.7	16.4
S4	PLC	0.1	- 400	75	1.2	32	3.3	76.7	52.4	31.1	11.3	19.8

TABLE 2. F. PIAZZA et al.

Material	Water CA (º)	E_S (mJ m^{-2})	E_p (mJ m^{-2})	E_δ (mJ m^{-2})	References
Ta-C:H (at 0.5 mTorr)	77.5-82.3	25.3-30.6	8.6-14.2	13.9-22	This work
Ta-C:H (from ion beam)	77-80	41.5	10.5	31	[35]
ta-C from FCVA	75-80		9-13	31.0-31.7	[42,54,55,56]
NCD	73±3		4.4	45.6	[57]
a-C:H (from polymer precursor)	88.1-91.7	25.3	1.7-3.8	21.1-37.3	[29]
Ta-C:H (at 0.9 mTorr)	75.8-77.8	29.2-31.7	11.1-12.7	16.4-20.4	This work
a-C:H (1.7-1.8 g/cm^3 mass-density)	71.3-74.4	32-34	12.7-15.2	18.7-19.5	This work
Low mass-density (1.2 g/cm^3) a-C:H	75.8-76.7	31-32.1	11.2-11.5	19.5-20.9	This work
a-C:Fe and a-C:Al from FCVA		25.3			[42]
a-C:H from PECVD		40-44			[36,37,38 , 52,53]

References

[1] J. Robertson, Materials Science and Engineering R 37 (2002) 129.

[2] X. Xiao, J. Birell, J.E. Gerbi, O. Auciello, J.A. Carlisle, J. Appl. Phys. 96 (2004) 2232.

[3] F. Piazza, J.A. González, R. Velásquez, J. De Jesús, S.A. Rosario, G. Morell, Diamond Relat. Mater. 15 (2006) 109.

[4] F. Piazza, G. Morell, Diamond Relat. Mater., 16 (2007) 1950.

[5] F. Piazza, F. Solá, O. Resto, G. Morell, L. Fonseca, Diamond Relat. Mater, submitted.

[6] A.C. Ferrari, Surf. Coat. Technol. 180-181 (2004) 190.

[7] M.F. Doerner, R.L. White, MRS Bull 28 (1996).

[8] B. Bhushan, Diamond Relat. Mater. 8 (1999) 1985.

[9] J. Robertson, Thin Solid Films 383 (2000) 81.

[10] P. Goglia, J. Berkowitz, J. Hoehn, A. Xidis, L. Stover, Diamond Relat. Mater. 10 (2001) 271.

[11] J.P. Sullivan, T.A. Friedmann, K. Hjort, MRS Bull. 26 (2001) 309.

[12] F. Piazza, D. Grambole, L. Zhou, F. Talke, C. Casiraghi, A.C. Ferrari, J. Robertson, Diamond Relat. Mater. 13 (2004) 1505.

[13] F. Piazza, D. Grambole, D. Schneider, C. Casiraghi, A.C. Ferrari, J. Robertson, Diamond Relat. Mater. 14 (2005) 994.

[14] C. Morsbach, C. Dubarry, M. Gabriel, M. Hoyer, S. Knappmann, F. Piazza, J.Robertson, R. Vullers, H.H. Gatzen, IEE Proc. Sci. Meas. Technol. 150 (2003) 203.

[15] K.R. Roy, K.R. Lee, J. Biomedical Mater. Res. B: Appl. Biomaterials, published online 6 February 2007 in Wiley InterScience (www.interscience.wiley.com). DOI: 10.1002/jbm.b.30768.

[16] S. Ramachandran, L. Tao, T. H. Lee, S. Sant, L. J. Overzet, M. J. Goeckner, M. J. Kim, G. S. Lee, and W. Hu, J. Vac. Sci. Technol. B 24 (2006) 2993.

[17] H.H. Gatzen, M. Beck, Tribol. Int. 36 (2003) 279.

[18] S. Cho, I. Chasiotis, T.A. Friedmann, J. Micromechanics Microengineering 15 (2005) 728.

[19] H.W. Liu, B. Bhushan, J. Vac. Sci. Technol., A 21 (2003) 1528.

[20] D.H.C. Chua, W.I. Milne, D. Sheeja, B.K. Tay, D. Schneider, J. Vac. Sci. Technol., B 22 (2004) 2680.

[21] P.D. Maguire, J.A. McLaughlin, T.I.T. Okpalugo, P. Lemoine, P. Papakonstantinou, E.T. McAdams, M. Needham, A.A. Ogwu, M. Ball, G.A. Abbas, Diamond Relat. Mater. 14 (2005) 1277.

[22] M. Weiler, S. Sattel, T. Giessen, K. Jung, H. Ehrhardt, V.S. Veerasamy, J. Robertson, Phys. Rev. B 53 (1996) 1594.

[23] M. Weiler, K. Lang, E. Li, J. Robertson, Appl. Phys. Lett. 72 (1998) 1314.

[24] N.A. Morrison, S. Muhl, S.E. Rodil, A.C. Ferrari, M. Nesladek, W.I. Milne, J. Robertson, Phys. Stat. Sol. (a) 172 (1999) 79.

[25] F. Piazza, Int. J. Refractory Metals and Hard Materials, 24 (2006) 39.

[26] F. Piazza, O. Resto, G. Morell, J. Appl. Physics, 102 (2007) 013301.

[27] H. Hofsaass, H. Feldermann, R. Merk, M. Sebastian, C. Ronning, Appl. Phys. A 66 (1998) 153.

[28] E. Lugscheider, K. Bobzin, M. Mfller, Thin Solid Films 355–356 (1999) 367.

[29] X.B. Yan, T. Xu, S.S. Yue, H.W. Liu, Q.J. Xue, S.R. Yang, Diamond Relat. Mater. 14 (2005) 1342.

[30] A. Erdemir, Surf. Coat. Technol. 146 (2001) 292.

[31] A. Erdemir, Trib. Int. 37 (2004) 1005.

[32] P.B. Leezenberg, W.H. Johnston, G.W. Tyndall, J. Appl. Phys. 89 (2001) 3498.

[33] H. Schift, A. Kristensen, Nanoimprint Lithography, in Springer Handbook of Nanotechnology, Bhushan Editor, Springer, 2006, p. 239-278.

[34] S. Adachi, T. Arai, K. Kobayashi, J. Appl. Phys. 80 (1996) 5422.

[35] V.S. Veerasamy, H.A. Luten, R.H. Petrmichl, S.V. Thomsen, Thin Solid Films 442 (2003) 1.

[36] R. Memming, H.J. Tolle, P.E. Wierenga, Thin Solid Films 143 (1986) 31.

[37] R.S. Butter, D.R. Waterman, A.H. Lettington, R.T. Ramos, E.J. Fordham, Thin Solid Films 311 (1997) 107.

[38] M. Grischke, A. Hieke, F. Morgenweck, H. Dimingen, Diamond Relat. Mater. 7 (1998) 454.

[39] Y. Mitsuya, H. Zhang, S. Ishida, Trans. ASME 123 (2001) 188.

[40] N.V. Novikov, S.I. Khandozhko, V.M. Perevertailo, L.Yu. Ostrovskaya, A.G. Gontar, O.B. Loginova, Diamond Relat. Mater. 7 (1998) 1263.

[41] K. Trojan, M. Grischke, H. Dimigen, Phys. Status Solidi, A Appl. Res. 145 (1994) 575.

[42] J.S. Chen, S.P. Lau, B.K. Tay, G.Y. Chen, Z. Sun, Y.Y. Tan, J. Appl.Phys. 89 (2001) 7814.

[43] A. Golanski, F. Piazza, J. Werckmann, G. Relihan, S. Schulze, J. Appl. Phys. 92, 3662 (2002).

[44] F. Piazza, D. Grambole, F. Herrmann, G. Relihan, M.F. Barthe, P. Desgardin, A. Golanski, Mat. Res. Soc. Symp Proc. 675, W10.3.1 (2001).

[45] F. Piazza, A. Golanski, S. Schulze, G. Relihan, Appl. Phys. Letters 82 (2003) 358 (2003).

[46] F. Piazza, S. Schulze, G. Relihan, A. Golanski, Diamond Relat. Mater. 12 (2003) 942.

[47] D.K. Owens, R.C. Wendt, J. Appl. Polym. Sci. 13 (1969) 1741.

[48] A.C. Ferrari, J. Robertson, Phys. Rev. 64 (2001) 075414.

[49] C. Casiraghi, F. Piazza, A.C. Ferrari, D. Grambole, J. Robertson, Diamond Relat. Mater. 14 (2005) 1098.

[50] S. Pisana, C. Casiraghi, A.C. Ferrari, J. Robertson, Diamond Relat. Mater., 15 (2006) 898.

[51] C. Maréchal, A. Zeinert, K. Zellama, E. Lacaze, M. Zarrabian, G. Turban, Solid State Comm. 109, 23 (1999).

[52] M.L. Wu, K. Howard, K. Grannen, J. Gui, G.C. Rauch, P.J. Sides, Thin Solid Films 377 (2000) 249.

[53] I.Y. Kim, S.H. Hong, A. Consoli, J. Benedikt, A. von Keudell, J. Appl. Phys. 100 (2006) 053302.

[54] H. Han, F. Ryan, M. McClure, Surf. Coat. Technol. 120-121 (1999) 579.

[55] D.H.C. Chua, K.B.K. Teo, T.H. Tsai, W.I. Milne, D. Sheeja, B.K. Tay, D. Schneider, Appl. Surface Science 221 (2004) 455.

[56] B.K. Tay, D. Sheeja, S.P. Lau, J.X. Guo, Diamond Relat. Mater. 12 (2003) 2072.

[57] L. Ostrovskaya, V. Perevertailo, V. Ralchenko, A. Saveliev, V. Zhuravlev, Diamond Relat. Mater. 16 (2007) 2109.

[58] J.O. Hansen, R.G. Copperthwaite, T.E. Derry, J.M. Pratt, J. Colloid, Interface Sci. 130 (1989) 347.

[59] L.Yu Ostrovskaya, V. Perevertailo, V. Ralchenko, A. Dementjev, O. Loginova, Diamond Relat. Mater. 11 (2002) 845.

[60] T. Halicioglu, Surf. Sci. Lett. 259 (1991) L714.

[61] G. Kern, J. Hafner, G. Kresse, Surf. Sci. 366 (1996) 464.

[62] J. Ristein, Diamond Relat. Mater. 9 (2000) 1129.

[63] J. Cui, J. Ristein, M. Stammler, K. Janischowsky, G. Kleber, L. Ley, Diamond Relat. Mater. 9 (2000) 1143.

[64] Y.M. Wang, K.W. Wong, S.T. Lee, M. Nishitani-Gamo, I. Sakaguchi, K.P. Loh, T. Ando, Diamond Relat. Mater. 9 (2000) 1582.

[65] L.Yu. Ostrovskaya, Vacuum 68 (2003) 219.

[66] M. Grischke, K. Bewilogua, K. Trojan, H. Dimigen, Surf. Coat. Technol. 74-75 (1995) 739.

[67] C.W. Chen, J. Robertson, J. Non Cryst. Solids 227/228 (1998) 602.

[68] J.J. Dong, D.A. Drabold, Phys. Rev. B 57 (1998) 15591.

[69] R. Haerle, G. Galli, A. Baldereschi, Appl. Phys. Lett. 7 (1999) 1718.

[70] P. Kelires, J. Non Cryst. Solids 230 (1998) 597.

[71] M. Kaukonen, R.M. Nieminen, S. Poykko, Phys. Rev. Lett. 87 (1999) 5346.

[72] C.W. Chen, J. Robertson, Diamond Relat. Mater. 15 (2006) 936.

[73] C.A. Davis, K.M. Knowles, G.A.I. Amaratunga, Phys. Rev. Lett. 80 (1998) 3280.

[74] M. P. Siegal, J. C. Barbour, P. N. Provencio, D. R. Tallant, and T. A. Friedmann, Appl. Phys. Lett. 73 (1998) 759.

[75] M. P. Siegal, P. N. Provencio, D. R. Tallant, R. L. Simpson, B. Kleinsorge, W. I. Milne, Appl. Phys. Lett. 76 (2000) 2047.

[76] A. LiBassi, A. C. Ferrari, V. Stolojan, B. K. Tanner, J. Robertson, and L. M. Brown, Diamond Relat. Mater. 9 (2000) 771.

[77] D.M. Gruen, Annu. Rev. Mater. Sci. 29 (1999) 211.

[78] E.V. Gribanova, A.N. Zhukov, I.E. Antonyuk, C. Benndorf, E.N. Baskova, Diamond Relat. Mater. 9 (2000) 1.

[79] L.Yu. Ostrovskaya, A.P. Dementiev, I.I. Kulakova, V.G. Ralchenko, Diamond Relat. Mater. 14 (2005) 486.

[80] V.M. Perevertailo, L.Yu. Ostrovskaya, O.B. Loginova, Proceedings of the fourth International Symposium on Diamond Films and Related Materials, Kharkov, Ukraine, 1999, p. 197.

[81] S. Arai, K. Tsujimoto, S. Tachi, Jpn. J. Appl. Phys. 31 (1992) 2011.

[82] A.M. Wrobel, in: K.L. Mittal (Ed.), Physicochemical Aspects of Polymer Surfaces, 1, Plenum, New York, 1981, pp. 197–215.

[83] G.J. Wan, P. Yang, Ricky K.Y. Fu, Y.F. Mei, T. Qiu, S.C.H. Kwok, Joan P.Y. Ho, N. Huang, X.L. Wu and Paul K. Chu, Diamond Relat. Mater.,15 (2006), 1276.

[84] P. Yang, J.Y. Chen, Y.X. Leng, H. Sun, N. Huang, P.K. Chu, Surf. Coat. Technol. 186 (2004) 125.